Heliyon 9 (2023) e21774

Contents lists available at ScienceDirect

Heliyon

journal homepage: www.cell.com/heliyon

Effectiveness of anti-erythropoietin producing Hepatocellular receptor Type-A2 antibody in pancreatic cancer treatment

Fu-Ling Chang [a], Keng-Chang Tsai [b,c], Tsai-Yu Lin [d], Chen-Wei Chiang [e], Shiow-Lin Pan [d,e,f,g,h,*,1], Yu-Ching Lee [c,d,e,f,**,1]

[a] *Ph.D. Program for Cancer Molecular Biology and Drug Discovery, College of Medical Science and Technology, Taipei Medical University and Academia Sinica, Taipei, Taiwan*
[b] *National Research Institute of Chinese Medicine, Ministry of Health and Welfare, Taipei, Taiwan*
[c] *Ph.D. Program in Medical Biotechnology, College of Medical Science and Technology, Taipei Medical University, Taipei, Taiwan*
[d] *Ph.D. Program for Cancer Molecular Biology and Drug Discovery, College of Medical Science and Technology, Taipei Medical University, Taipei, Taiwan*
[e] *Ph.D. Program in Drug Discovery and Development Industry, College of Pharmacy, Taipei Medical University, Taipei, Taiwan*
[f] *TMU Research Center of Cancer Translational Medicine, Taipei Medical University, Taipei, Taiwan*
[g] *Graduate Institute of Cancer Biology and Drug Discovery, College of Medical Science and Technology, Taipei Medical University, Taipei, Taiwan*
[h] *TMU Research Center for Drug Discovery, Taipei Medical University, Taipei, Taiwan*

A R T I C L E I N F O

Keywords:
Erythropoietin-producing hepatocyte receptor type-A2
Pancreatic cancer
Phage display
EphA2 degradation
Improved effects

A B S T R A C T

Erythropoietin-producing hepatocyte receptor type A2 (EphA2) is a tyrosine kinase that binds to ephrins (e.g., ephrin-A1) to initiate bidirectional signaling between cells. The binding of EphA2 and ephrin-A1 leads to the inhibition of Ras-MAPK activity and tumor growth. During tumorigenesis, the normal interaction between EphA2 and ephrin-A1 is hindered, which leads to the overexpression of EphA2 and induces cancer. The overexpression of EphA2 has been identified as a notable tumor marker in diagnosing and treating pancreatic cancer. In this study, we used phage display to isolate specific antibodies against the active site of EphA2 by using a discontinuous recombinant epitope for immunization. The therapeutic efficacy and inhibition mechanism of the generated antibody against pancreatic cancer was validated and clarified. The generated antibodies were bound to the conformational epitope of endogenous EphA2 on cancer cells, thus inducing cellular endocytosis and causing EphA2 degradation. Molecule signals pAKT, pERK, pFAK, and pSTAT3 were weakened, inhibiting the proliferation and migration of pancreatic cancer cells. The humanized antibody hSD5 could effectively inhibit the growth of the xenograft pancreatic cancer tumor cells BxPc-3 and Mia PaCa-2 in mice, respectively. When antibody hSD5 was administered with gemcitabine, significantly improved effects on tumor growth inhibition were observed. Based on the efficacy of the IgG hSD5 antibodies, clinical administration of the hSD5 antibodies is likely to suppress tumors in patients with pancreatic cancer and abnormal activation or overexpression of EphA2 signaling.

* Corresponding author. Graduate Institute of Cancer Biology and Drug Discovery, College of Medical Science and Technology, Taipei Medical University #250 Wu-Hsing Street, Taipei, Taiwan 110.
** Corresponding author. TMU Research Center of Cancer Translational Medicine, Taipei Medical University, #250 Wu-Hsing Street, Taipei, Taiwan 110.
E-mail addresses: slpan@tmu.edu.tw (S.-L. Pan), ycl@tmu.edu.tw (Y.-C. Lee).
[1] These authors contribute equally in this work.

https://doi.org/10.1016/j.heliyon.2023.e21774
Received 15 February 2023; Received in revised form 23 October 2023; Accepted 27 October 2023
Available online 4 November 2023

1. Introduction

Erythropoietin-producing hepatocyte receptors (Ephs) are proteins belonging to the family of tyrosine kinases. These proteins were identified in studies exploring the function of organisms and were classified based on structural and functional characteristics [1]. The main biological function of Eph receptor proteins is generating activation signals by binding ligands (such as ephrins). Studies have demonstrated that the Eph–ephrin system drives several types of cells to alter cell motility and morphology [2]. With some exceptions, nine type-A EphA receptors (EphA1–A9) interact and bind to five glycosylphosphatidylinositol (GPI) anchor-linked type-A ephrin ligands (A1–A5), whereas five type-B Eph receptors bind to three type-B ephrin ligands (B1–B3) with transmembrane proteins [3]. Several organismal functions are associated with the Eph–ephrin system, mainly transmitting signals created through receptor–ligand interaction. Numerous studies have demonstrated that the Eph–ephrin system affects tumorigenesis, angiogenesis, cancer immunity, cancer metastasis, and tumor stem cell proliferation [4]. However, each member of this complex cellular communication system can either have a negative or positive effect on tumorigenesis, depending on the type of cancer; studies have demonstrated that Ephs can also drive ligand-independent signaling, which may be the key to tumorigenesis [2].

Erythropoietin-producing hepatocyte receptor type A2 (EphA2) is a member of the Eph family of tyrosine kinases. It is a highly conserved protein that exhibits 90 % protein sequence similarity with the corresponding protein in mice [5]. EphA2 binds to various membrane-immobilized ephrins or presents freely in the serum. The EphA2–ephrin-A1 signaling pathway is the most studied and crucial in regulating cellular tissue function. Unlike other receptor tyrosine kinase proteins, Eph receptors such as EphA2 usually have tumor-suppressive effects, and their binding to ephrins (ephrin-A1) results in the inhibition of Ras–mitogen-activated protein kinase activity [2]. However, during tumorigenesis, the extent of regular interactions between EphA2 and ephrin-A1 decreases, resulting in the overexpression of EphA2, which is associated with the occurrence, migration, and invasion of tumors [6]. Abnormal EphA2 expression can be detected in various cancers, such as melanoma, lung, brain, and pancreatic cancer (PDAC) [7–10]. Studies have discovered that the phosphorylation of EphA2 determines whether EphA2 acts as a tumor promoter or suppressor. EphA2 can act as a tyrosine kinase and block AKT activation through ephrin-A1 stimulation, thus inhibiting the growth of cancer cells. Conversely, this interaction is blocked in cancer cells when EphA2 is overexpressed and not activated by ephrin-A1; therefore, it initiates the cancer-promoting AKT/mammalian target of rapamycin 1 signaling pathway [11]. The overexpression of EphA2 occurs in cancer cells in a ligand-independent manner to regulate and promote tumor growth [12], and ligand-independent EphA2 signals synergize with the signals transmitted by epidermal growth factor (EGF) receptors to promote tumor growth and invasion [13]. Therefore, the availability of ephrins during tumor development determines the functional direction of EphA2. Thus, converting or neutralizing the EphA2-regulated tumor growth response through the binding of inhibitors (e.g., antibodies) is a crucial research topic.

The gene expression of EphA2 is considerably elevated in PDAC tissues and it adversely affects the survival rate of patients. Studies have observed the high expression of EphA2 in 92 % of PDAC samples; it can be detected during the pretumor stage and increases as the disease progresses [10,14]. PDAC has no apparent symptoms in the early stage, and the overall 5-year survival rate is approximately 8 % [15]. Treatments for PDAC include surgical resection, chemotherapy, and radiation therapy. However, the success rate of these treatments is limited, and recurrence occurs in most cases. No clinically effective target drug for PDAC exists. Therefore, effective drugs for treating PDAC must be developed. Therefore, this study prepared anti-EphA2 antibodies by directly targeting the active site of EphA2 to induce an effective immune response to the highly conserved protein EphA2 in chickens. The isolated antibodies have excellent specificity and a strong neutralization ability for EphA2, and they can precisely and effectively inhibit tumors by binding to EphA2.

2. Materials and methods

2.1. Cell culture and animal immunization

The human PDAC cell lines AsPc-1, BxPc-3, Panc-1, and Mia PaCa-2 were purchased from the American Type Culture Collection (ATCC) (Manassas, VA, USA). All cell lines were cultured according to ATCC standard protocols and incubated at 37 °C in a humidified atmosphere of 5 % CO_2.

Female white leghorn (*Gallus domesticus*) chickens and nonobese diabetic mice with severe combined immunodeficiency (NOD/SCID) were purchased from the National Laboratory Animal Center, Taiwan, and were maintained in the Taipei Medical University animal facility.

2.2. Bioinformatics analysis

To investigate the association between EphA2 gene expression and PDAC occurrence, we used the Gene Expression Profiling Interactive Analysis (GEPIA; http://gepia.cancer-pku.cn) database to analyze the difference in EphA2 expression in clinical cancer samples and normal samples and to analyze the correlation between EphA2 expression and the PDAC survival rate [16].

2.3. Antibody library construction and biopanning

Based on the complex protein structure of ephrinA1–EphA2 (Protein Data Bank [PDB] ID: 3CZU), we designed a peptide immunogen for the EphA2 target molecule; the peptide immunogen (EphA2pep) contains Epitope 1, GWDLMQNIMNDMPIYMYSV, and

Epitope 2, VSSDFEARHV, which were linked together by using a linker GGGGGGS. EphA2pep contains six consecutive repetitive sequences. After gene synthesis (GENEWIZ), it was constructed on a pET21a vector (Novagen) and transformed into the *Escherichia coli* BL-21 (DE3) strain for its expression as a recombinant protein. After purification using Ni^{2+}-charged sepharose (GE Healthcare Life Sciences), the recombinant EphA2pep protein was used for animal immunization. Female white leghorn chickens were immunized through intramuscular injection of 50 μg of recombinant EphA2pep protein in 500 μl PBS mixed with a 500 μl adjuvant each time. During the immunization, we used Freund's complete adjuvant (Sigma-Aldrich) the first time and Freund's incomplete adjuvant (Sigma-Aldrich) all other times. The immunization schedule comprised four immunizations performed at intervals of 7 days. The spleens of the chickens were harvested 7 days after the final immunization to construct an scFv antibody library. The library was constructed following published protocols, with minor modifications [17].

For panning, the 1 μg recombinant EphA2 protein was pre-coated onto the well of a microtiter plate at 4 °C overnight. The EphA2 protein was removed the next day, and the well was blocked with 3 % BSA at room temperature for 1 h. Then, the 100 μl of recombinant library phage solution (10^{11} phage particles) was added to the well and incubated at room temperature for 2 h. Unbound phages in the supernatants were removed, and the well was washed through pipetting with phosphate-buffered saline with 0.05 % Tween 20 (PBST) 10 times. Subsequently, bound phages were eluted with 100 μl of 0.1 M HCl–glycine (pH 2.2)/0.1 % BSA elution buffer and neutralized with 6 μl of 2 M Tris base buffer. The eluted phages were immediately used to infect the *E. coli* ER2738 strain for recombinant phage amplification. Amplified phages were precipitated and recovered through a previous method [18] and were used in the next round of panning. The panning procedure was repeated four times to enrich anti-EphA2 binding phages efficiently. After panning, the library DNA was purified and transformed into the *E. coli* strain TOP 10F' (Invitrogen, a nonsuppressor strain) for scFv expression. The expressed scFv was further purified with Ni^{2+}-charged sepharose following the manufacturer's instructions (GE Healthcare Life Science).

2.4. Sequence analysis

To sequence the scFv clones of interest, we used the ompseq primer (5′-AAGACAGCTATCGCGATTGCAGTG-3′) complementary to the outer membrane protein A (ompA) signal sequence upstream of the light chain variable region. Next, the website International ImMunoGeneTics information system/V-QUEry and Standardization (http://imgt.org) were used to compile and analyze the sequence data based on the germline genes.

2.5. Enzyme-linked immunosorbent assay

The recombinant EphA2 protein (0.1 μg/well) was coated onto the microtiter plate wells at 4 °C overnight. The wells were blocked with 100 μl of 5 % skim milk, and scFv or phage was added at room temperature for 1 h. After the wells were washed with PBST, the bound scFv or phage was then detected and developed using 50 μl of horseradish peroxidase (HRP)-conjugated goat anti-chicken light chain antibodies (Bethyl Laboratories) or HRP-conjugated anti-M13 antibodies (GE Healthcare Life Science). Finally, 50 μl of substrate 3,3′,5,5′-tetramethylbenzidine dihydrochloride (TMB) was added for signal development. The reaction was stopped by adding 25 μl of 1 N HCl, and absorbance was measured by determining optical density (OD) at 450 nm.

2.6. Western blotting and immunoprecipitation assay

The 1 μg of recombinant EphA2 protein was transferred onto nitrocellulose membranes (GE Healthcare Life Sciences) after electrophoresis using sodium dodecyl sulfate–polyacrylamide gel (SDS-PAGE) or native-polyacrylamide gel (Native-PAGE), and the membranes were incubated with using purified scFv antibodies to determine binding reactivity. The membranes were blocked with 5 % skim milk and then incubated with 1 μg/ml of scFv at room temperature for 1 h. After washing with PBST, the membranes were detected and developed using HRP-conjugated goat anti-chicken light chain antibodies. Finally, the 3,3′-diaminobenzidine substrate was added for color development until the desired color intensity was reached.

For the immunoprecipitation assay, 300 μg of each PDAC cell lysate was incubated with 50 μg anti-EphA2 scFv in 150 μl of PBS (scFv was fused with a His tag) at 4 °C overnight. The next day, 350 μl PBS and 30 μL of Ni^{2+}-charged sepharose were added to the mixture and incubated for 1 h at 4 °C. After three rounds of washing with PBS, the scFv-bound sepharose beads were resuspended in 50 μL of PBS buffer. Subsequently, the sepharose solution was denatured at 95 °C for 10 min and analyzed using SDS-PAGE. After the proteins were transferred to a polyvinylidene fluoride membrane, the membrane was detected using the 1 μg/ml anti-EphA2 antibody (R&D Systems) or anti-His (Proteintech Group) antibody at 4 °C overnight. The next day, after washing with PBST, the membrane was incubated with HRP-conjugated secondary antibody (Jackson ImmunoResearch Laboratories). Finally, the chemiluminescence substrate was added for luminal signal detection.

2.7. Flow cytometry analysis

Four PDAC cells, AsPc-1, BxPc-3, Panc-1, and Mia PaCa-2 with endogenous EphA2 molecule expression, were analyzed through flow cytometry to determine the binding reactivity of indicated scFvs. Freshly prepared cancer cells were harvested and washed twice with PBS. Then, individual 1 μg/ml of scFv was added and incubated at room temperature for 1 h. Bound scFv was visualized using goat anti-chicken light chain antibodies and donkey anti-goat antibodies conjugated with fluorescein isothiocyanate (FITC; Jackson ImmunoResearch Laboratories). An irrelevant scFv was used as the negative control, and commercially available goat anti-EphA2

antibodies were used as the positive control (R&D Systems) in the assay. The results were analyzed using a FACS can flow cytometer (BD Biosciences, Systems and Reagents).

To detect the binding specificity of scFv, 293T cells were transformed with EphA1-A8 plasmids individually for overexpression of different EphA molecules. The cell line was freshly prepared and washed with FACS buffer (2 % FBS in PBS). The cells were seeded at 1×10^5 cells/well into a 96-well U-bottom plate and incubated with scFv for 1 h at 4 °C. After the plate was washed with FACS buffer, the anti-hemagglutinin (HA) antibody was added for scFv binding detection (scFv was fused with a HA tag) and subsequently developed using an FITC-conjugated secondary antibody. Finally, the cell binding signal was analyzed using a FACScan flow cytometer.

2.8. Cell proliferation assay

PDAC cell proliferation was measured using a 3-(4,5-dimethylthiazol-2-yl)-5-(3-carboxymethoxyphenyl)-2-(4-sulfophenyl)-2H-tetrazolium (MTS) Cell Proliferation Assay Kit (Promega). The cells were seeded in a 96-well culture plate at a density of 5000 cells/well for attachment. Then, scFv at various concentrations was added to the cell culture and incubated for 5 days. Finally, 40 μl of MTS and phenazine methosulfate mixture solutions were added and incubated for 90 min for development. After the 25 μl of SDS reagent was added to stop the reaction, the absorbance of each well was measured by determining the OD at 490 nm.

2.9. Cell migration and scratch wound healing assay

PDAC cells were seeded at 5×10^4 cells/well in a 24-well Transwell cell migration plate (Corning) and incubated with 20 μM of scFv for 2 days. The assay added 1 mg/ml of recombinant ephrin-A1 (Sino Biological) as a positive control. After scFv treatment, the cells were fixed with frozen 100 % methanol for 10 min and stained with 0.01 % crystal violet for 1 h at room temperature. After the pate was washed with ddH_2O, the upper-layer cells were removed using cotton swabs. Cell staining was imaged using a microscope and analyzed using ImageJ.

PDAC cells were seeded in a 6-well culture plate for the scratch wound healing assay. The seeded cells in the well were scratched with a pipette tip to simulate a wound. After treatment with 20 μM of scFv and incubation for 36 or 72 h, the cells were imaged using a microscope. The wound areas were analyzed using ImageJ.

2.10. Molecule signaling

The BxPc-3 and Mia PaCa-2 cells were each seeded in 6-well culture plates. They were treated with scFv antibodies at indicated concentrations and incubated for 24 h to investigate molecular signaling. The cells were collected and lysed using 200 μl of lysis buffer [50 mM Tris–HCl (pH 7.5), 50 mM NaCl, 5 mM ethylenediaminetetraacetic acid, and 1 % Triton X-100], and a mixture of proteinase inhibitors (Roche Applied Science) was added. The protein concentration of the cell lysate was measured through the Coomassie Plus (Bradford) Protein Assay (Thermo Fisher Scientific). Samples were run on reducing SDS-PAGE for Western blotting analysis and were detected using antibodies against *p*-EphA2, EphA2, *p*-AKT, AKT, *p*-ERK, ERK, *p*-FAK, FAK, p-STAT3, STAT3, Lamp1, Lamp2 (Cell Signaling Technology), and β-actin (GeneTex).

2.11. Antibody internalization assay

BxPc-3 cells were seeded on cover glasses placed in the wells of a 6-well culture plate. The BxPc-3 seeded glass slides were incubated with 1 μg/ml of ephrin A1-Fc (Sino Biological) or 1 μg/ml of IgG hSD5 for 1 h at 37 °C or 4 °C. After washing with PBS, the cells were fixed with 100 % ice methanol for 10 min. Next, the cells were stained with an FITC-conjugated anti-human Fc antibody and were subsequently mounted with ProLong Diamond Antifade Mountant comprising 4',6-diamidino-2-phenylindole for nuclear counterstaining (Invitrogen). The cells were imaged using a confocal microscope (Leica Microsystems).

2.12. Tumor xenograft model

The freshly prepared BxPc-3 and Mia PaCa-2 cancer cells were harvested during the log growth phase and resuspended in PBS for tumor implantation. Each NOD/SCID mouse was subcutaneously inoculated with cancer cells (5×10^6 to BxPc-3 and 1×10^7 to Mia PaCa-2) for tumor formation. The tumor size was measured twice weekly, and the volume was calculated as follows: $V = 0.5lw^2$, where l = the length and w = the width. When the tumor size was approximately 100 mm^3, animals were divided into groups that received (a) vehicle alone through intravenous injection (i.v.) once weekly (qwk), (b) control human IgG1 at 20 mg/kg through i.v. qwk, (c) and (d) hSD5 IgG1 at 2 or 20 mg/kg through i.v. qwk, (e) gemcitabine at 20 through i.v. twice weekly (biw), or (f) hSD5 IgG1 at 2 mg/kg through i.v. qwk combined with gemcitabine at 20 mg/kg through i.v. biw. At the end of the experiment, the antitumor effects were quantified by dividing the tumor volumes in the treatment groups by those in the control groups and multiplying them by 100 to represent tumor growth inhibition (TGI; %). The mice were also examined frequently for overt signs of adverse drug-related side effects.

2.13. Immunohistochemical staining

The pancreatic tissue microarray slide (US Biomax, PA483e) was used to detect and analyze the EphA2 expression of clinical samples. In the xenograft animal model, the excised BxPc-3 and Mia PaCa-2 tumors were fixed in formalin, embedded in paraffin, and sliced for immunohistochemical staining (IHC). Commercial antibodies (Cell signaling, Dako; Agilent Technologies; and Abcam) were used for staining the EphA2 molecule, cell proliferation marker Ki-67, and apoptosis marker cleaved caspase 3. The effects of staining were observed using a Zeiss Axioskop-2 microscope (Carl Zeiss).

2.14. Interaction residue definition

We used peptide enzyme-linked immunosorbent assay (ELISA) to identify the designed epitope on EphA2; the BSA-conjugated peptides EphA2pep_P1 (BSA-CGGGWDLMQNIMNDMPIYMYSV) and EphA2pep_P2 (BSA-CGGGGGGSVSSDFEARHV) each represent the two segments of the linear epitope designed on EphA2. EphA2pep_P1P2 (BSA-CGGGWDLMQNIMNDMPIYMYSVGGGGGGSVSS DFEARHV) represents the two linear epitope sequences connected by a linker. These peptides were synthesized and conjugated with BSA (Kelowna International Scientific). The BSA-conjugated peptides were individually coated on a 96-well microplate (2 μg/well) at 4 °C overnight. After the wells were blocked with 3 % BSA, 10 μg/ml of IgG hSD5 was added and incubated. Next, an HRP-conjugated anti-human Fc antibody was used to detect bound antibody. Finally, 50 μl of TMB substrate was added for development, and the reaction was stopped by adding 25 μl of 1 N HCl. Absorbance was measured by determining the OD at 450 nm.

A dot blot assay was used to detect the binding of IgG hSD5 to the synthesized peptides; 1 μL of individual peptides (1 mg/mL; in triplicate) were dropped on the NC membrane and maintained at RT for complete absorption. Blocking with 3 % BSA was performed at RT for 1 h. Then, IgG hSD5 (10 μg/mL) was added, and the reaction was allowed to proceed for 1 h at RT. After the membrane was washed, the HRP-conjugated anti-HA tag antibody was added, and the reaction was allowed to proceed for 1 h at RT. Lastly, DAB was used to initiate the coloration reaction.

2.15. Statistical analysis

The data are presented as mean ± standard error of the mean and were analyzed using GraphPad Prism (GraphPad Software). Statistical comparisons between groups were performed using one-way analysis of variance, which was followed by a post hoc Tukey's honest significant difference test. *P* values lower than 0.05 were considered significant (*$p < 0.05$, **$p < 0.01$, ***$p < 0.001$, ****$p < 0.0001$).

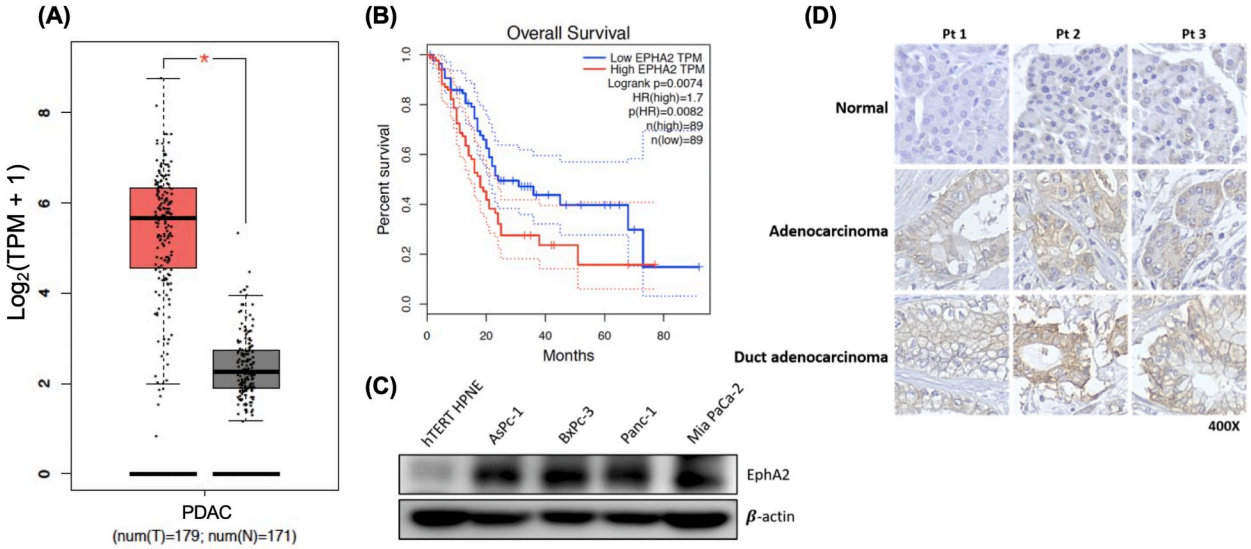

Fig. 1. Analysis of the correlation between EphA2 expression and PDAC. (A) Differences in the expression of the EphA2 gene in PDAC specimens (red bar) and normal specimen samples (gray bar) analyzed using the GEPIA database. (B) Correlation between EphA2 gene expression and survival in patients with PDAC. Patients with high EphA2 gene expression (red line) had lower survival rates than did those with low EphA2 gene expression (blue line). (C) The expression of EphA2 molecules in four PDAC cells, Panc-1, Mia PaCa-2, AsPc-1, BxPc-3, and one normal pancreatic endothelial cell, hTERT-HPNE, were analyzed using Western blotting. (D) The IHC staining was performed using tissue microarray to observe the differences in the expression of EphA2 molecules in clinical PDAC tissues and normal pancreatic tissues. *$p < 0.05$.

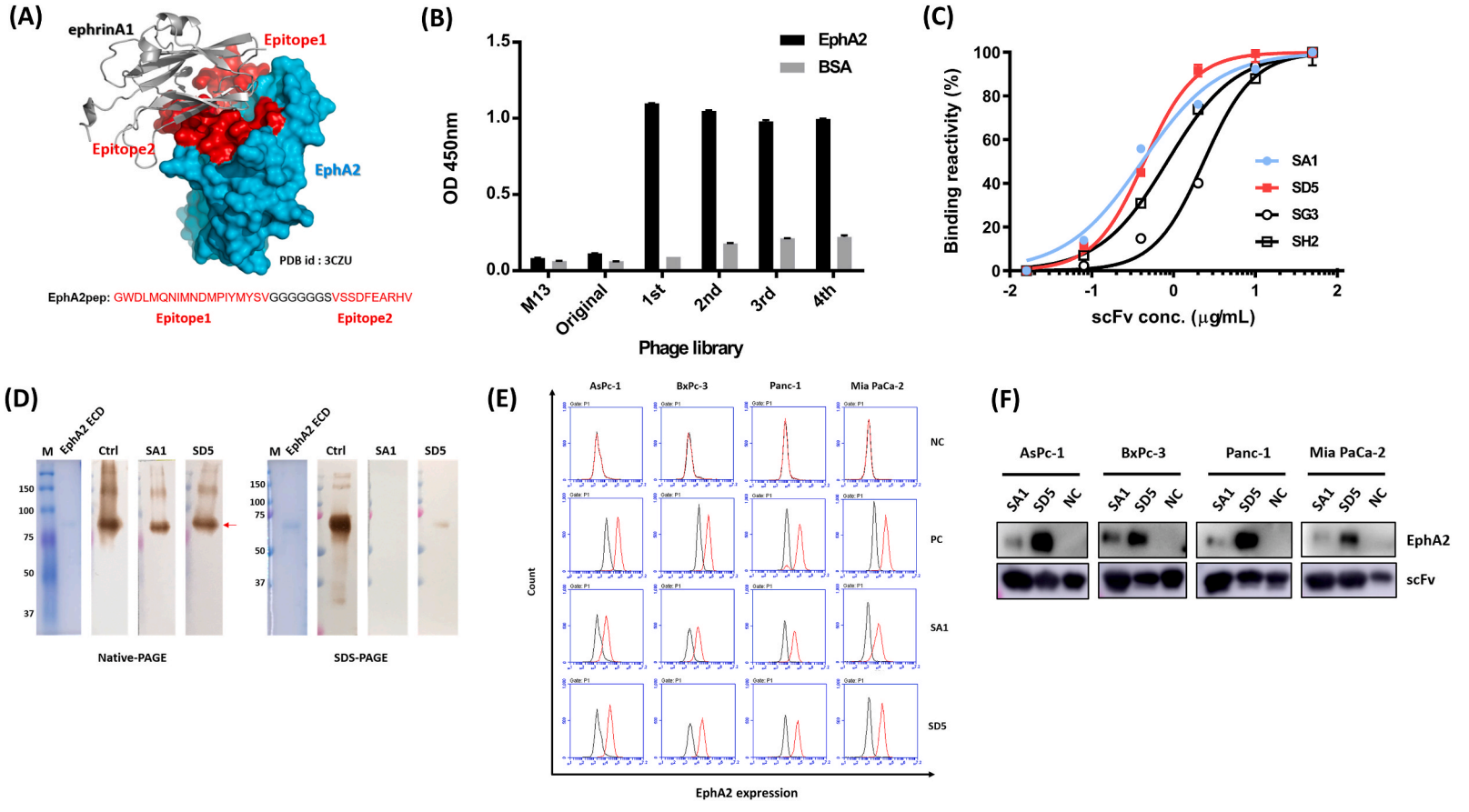

Fig. 2. Characterization of anti-EphA2 scFvs isolated using phage display technology. (A) On the basis of the X-ray crystal structure of PDB ID: 3CZU, the discontinuous antigenic peptide of the active site of EphA2 was designed; ephrin-A1 is gray, EphA2 is blue-green, and the red part is the two antigen peptide segments (Epitope1 and Epitope2) located on EphA2. The EphA2pep is the complete sequence design after linking of the two antigenic peptide segments. (B) The phage ELISA was used to test the binding reaction of the reamplified phage antibody library to the EphA2 recombinant protein after each round of panning, with "original" representing the original antibody library and "M13" representing the wild type phage. (C) Percentage of binding of the four representative scFv strains to EphA2 molecules at various test concentrations. (D) Western blotting was used to test the reaction of scFv SA1 and SD5 under reduced (SDS-PAGE) and normal (Native-PAGE) conditions to identify the EphA2 protein; Ctrl is the result of detection using commercial Ab. (E) Flow cytometry was used to analyze the response of scFv SA1 and SD5 in identifying endogenous EphA2 molecules on the four strains of PDAC cells. PC represents the use of commercial Ab to determine the expression of EphA2 on cancer cells; NC represents the control group without the addition of the antibody. (F) The scFv SA1 and SD5 were used to pull down the endogenous EphA2 molecules in the lysate by immunoprecipitation of the four strains of PDAC cells, and NC represents the irreverent scFv that did not exhibit any reaction.

3. Results

3.1. Expression and correlation of EphA2 in PDAC

One key to the success of targeted therapy is the specificity of the targeted cancer antigens. We used the GEPIA database to evaluate the performance of EphA2 molecules in PDAC. The red bar in Fig. 1A represents the cancer samples (n = 179), and the gray bar represents normal samples (n = 171); the genetic expression of EphA2 exhibited a meaningful increase in the PDAC samples. We also discovered that the cancer types with high expression of the EphA2 gene were cervical squamous cell carcinoma, colon adenocarcinoma, glioblastoma, ovarian serous cystadenocarcinoma, rectum adenocarcinoma, stomach adenocarcinoma, and thymoma (Supplementary Fig. 1). The involved organs of the digestive tract were the stomach, pancreas, and colorectum, suggesting a correlation between the expression of EphA2 and the digestive organs. Through the analysis of survival correlation (Fig. 1B), we discovered that patients with higher EphA2 gene expression (red line) exhibited lower survival rates. We used four PDAC cell lines AsPc-1, BxPc-3, Panc-1, Mia PaCa-2 and one normal pancreatic endothelial cell line hTERT-HPNE to compare the expression of EphA2 in cancer cells. All four PDAC cell lines exhibited higher expression of the EphA2 protein than did the control hTERT-HPNE cell line (Fig. 1C). In addition, using IHC of the tissue microarray, we discovered higher levels of EphA2 in the cell membranes of the clinical PDAC tissue specimens than in the normal pancreatic tissues (Fig. 1D).

3.2. Generation of anti-EphA2 scFv antibody by using phage display technology

We analyzed the structure of the complex protein (PDB ID: 3CZU) formed by EphA2 (blue-green) and ephrin-A1 (gray) (Fig. 2A). We expanded the binding site of ephrin-A1 to the range of 5 Å and determined the amino acids in the EphA2 molecule that may result in interactions. Based on this information, we created a peptide sequence with discontinuous fragments (red: Epitope 1 and Epitope 2), and a linker sequence (GGGGGGS) was used to link EphA2pep: GWDLMQNMNDMPIYMYSVGGGGGGSVSSDFEARHV. We immunized the chickens after expressing the 6-repetition peptide sequences as a recombinant protein (Supplementary Fig. 2). Subsequently, we constructed a highly complex library of scFv antibodies and isolated specific antibodies using phage display technology. We found that the number of bound phages increased by approximately 60-fold between the first and last rounds (data not shown), indicating that the specific binding strains were enriched by panning. In phage ELISA, the amplified phage library obtained after the first round of panning already contained enriched specific strains that exhibited considerable binding reactions to EphA2 compared with the original antibody library (original) and wild-type M13 phage (Fig. 2B). After gene sequencing, we serially diluted the four isolated representative scFvs to test the binding reaction to EphA2 (Fig. 2C). The EC_{50} values of scFv SA1 and SD5 were similar at 1.7 and 1.8 nM, and the EC_{50} values of scFv SG3 and SH2 were 33.6 and 94 nM, respectively; the difference in binding capacity resulted from the interaction of the CDR sequences of different antibodies on the EphA2 molecule.

3.3. Isolated scFvs can recognize the conformational epitope of endogenous EphA2 on cancer cells

We selected the scFv SA1 and SD5 with the best EC_{50} values for subsequent testing. By using Native-PAGE (red arrow), we determined that scFv SA1 and SD5 can recognize EphA2 in the native form but not in the denatured form, which indicates that the epitope recognized by scFvs is conformational (Fig. 2D). We used flow cytometry to test the binding reaction of scFv SA1 and SD5 to endogenous EphA2 molecules on the four strains of PDAC cells. The results indicate that the scFvs exhibited a significant binding response to the EphA2 molecules on cancer cells (Fig. 2E). To further explore the ability of the antibody to bind to the endogenous EphA2 molecule, we used scFv SA1 and SD5 to perform immunoprecipitation experiments on the cell lysates of the four strains of PDAC cells (Fig. 2F). Compared with the irrelevant scFv in the control group, which did not bind to EphA2, both scFv SA1 and SD5 captured free EphA2 molecules from the lysates of the four strains of PDAC cells, and the binding effect of scFv SD5 was superior to that of SA1.

3.4. Anti-EphA2 scFvs can inhibit the growth and migration of PDAC cells

We conducted a cell survival analysis assay (MTS assay) to observe the growth inhibitory effect of scFv SA1 and SD5 on the four PDAC cell lines by adding different concentrations of antibodies to the cell culture. By Day 5 of the antibody reaction, scFv SA1 exhibited an approximately 18%–24 % inhibitory effect on the cancer cell lines AsPc-1 and BxPc-3 (Fig. 3A). However, at a concentration of 20 μM, scFv SD5 inhibited the growth of three cell lines, AsPc-1, Panc-1, and Mia PaCa-2, by approximately 80 %. Additionally, it inhibited the growth of the cell line BxPc-3 by 58.5 %. Dose-dependent responses were observed at different antibody concentrations; this result indicates that the binding of scFv SD5 to EphA2 on the surface of PDAC cells can inhibit the growth of cancer cells. We also treated the normal pancreatic endothelial cell line hTERT-HPNE with the same conditions of scFv SD5 treatment. Due to the low expression of EphA2, the results showed that it did not produce a growth inhibition response similar to cancer cells (Supplementary Fig. 3).

Because the molecular regulation of EphA2 has been demonstrated to promote the migration of cancer cells, we used both the transwell migration assay and wound healing assay to determine whether scFv SA1 and SD5 inhibit the migration of PDAC cells. The results of the transwell migration assay are presented in Fig. 3B. The experimental responses of the cancer cells BxPc-3 and Mia PaCa-2 revealed that after treatment with scFv SA1 and SD5 at the dose of 20 μM for 2 days, both reduced the number of migrated cancer cells. Fig. 3C presents a quantitative graph illustrating the inhibitory effect of the antibody on the migration of the four strains of PDAC cells;

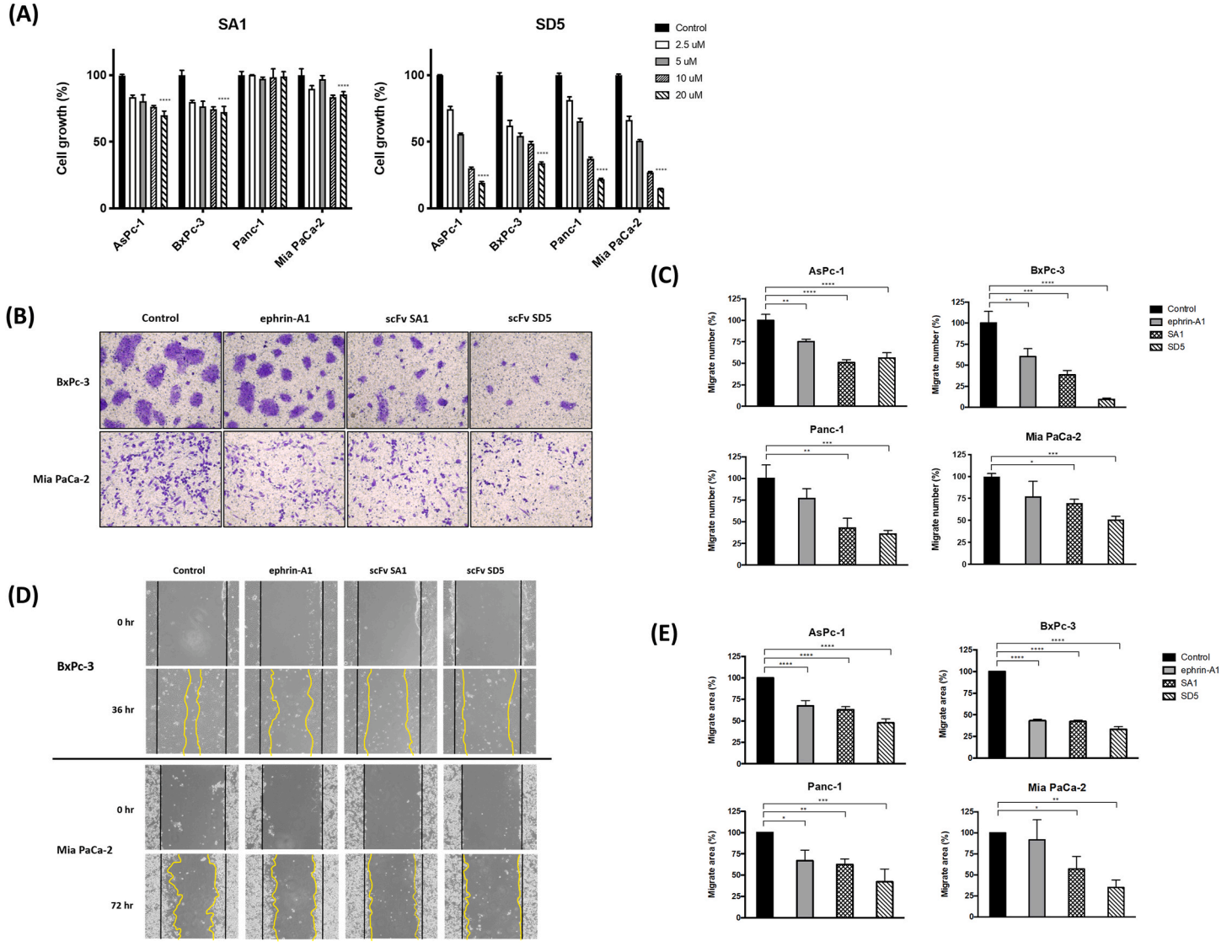

Fig. 3. Isolated scFvs can inhibit the proliferation and migration of PDAC cells. (A) The growth inhibitory effect of scFvs on the four strains of PDAC cells was tested under different concentrations. At indicated concentrations, scFv SA1 and SD5 interacted with the cancer cells for 5 days, and the effects on the growth of cancer cells were observed. (B) According to the experimental results for BxPc-3 and Mia PaCa-2 cells, treatment with scFv SA1 and SD5 in the transwell migration assay reduced the number of cancer cells that migrated through the porous membrane. (C) The quantified percentage was used to illustrate the migration inhibitory effect of scFvs on the four strains of PDAC cells in the transwell migration assay. (D) According to the experimental results for BxPc-3 and Mia PaCa-2 cells, treatment with scFv SA1 and SD5 in the wound healing assay inhibited the crawling reaction of the cancer cells. (E) The quantified percentage was used to illustrate the migration inhibitory effect of scFvs on the four strains of PDAC cells in the wound healing assay. $*p < 0.05$, $**p < 0.01$, $***p < 0.001$, $****p < 0.0001$.

the experimental results for scFv SD5 were better than those for scFv SA1. The scFv SD5 can inhibit the migration of the cancer cell lines Panc-1 and BxPc-3 by 65 % and 91 %, respectively. The results of the wound healing assay are presented in Fig. 3D. Based on the experimental reactions of the cancer cells BxPc-3 and Mia PaCa-2, both scFv SA1 and SD5 inhibited the crawling response of cancer cells after 36 and 72 h of treatment with scFv. Fig. 3E presents a quantitative graph illustrating the inhibitory effect of the antibody on the four strains of PDAC cells. The experimental results for scFv SD5 are superior to those of scFv SA1; scFv SD5 exhibited higher reactivity to the cancer cell lines Mia PaCa-2 and BxPc-3, and the inhibitory effects were 65 % and 67 %, respectively. Therefore, we selected scFv SD5 for the subsequent experiments.

3.5. Molecule signaling and endocytosis response after humanized IgG hSD5 treatment

To improve the clinical applicability of the antibodies, we performed the humanization of chicken-derived scFv SD5. Because the Ephs family molecules (EphA1–A8) have numerous roles in human cell physiology, the specificity of the isolated antibodies for EphA2 molecules must be determined. Using cells with overexpression of EphA1–A8 molecules, we demonstrated that humanized scFv hSD5 specifically binds to EphA2 molecules and does not exhibit cross-binding reactions to other family proteins (Fig. 4A). We observed changes in molecular signaling in cancer cells after the administration of scFv hSD5. The cancer cells BxPc-3 and Mia PaCa-2 degraded EphA2 molecules 6 h after the administration of scFv and exhibited a dose-dependent response. The lysosomal-associated proteins LAMP1 and LAMP2 also exhibited upregulated levels in the two cancer cell lines (Fig. 4B), which means that scFv hSD5 may enter the cell through endocytosis after acting on EphA2 and that the lysosome is involved in the degradation of the protein. After the two cancer cells lines of BxPc-3 and Mia PaCa-2 were treated with different concentrations of scFv hSD5 for 24 h, EphA2 was almost completely degraded, and the amount of pEphA2 also decreased (Fig. 4C). The signals pERK and pAKT, associated with cancer cell proliferation and metastasis, also exhibited a similar decrease. In the signals related to cancer cell survival and adhesion, a dose-dependent decrease was observed for both signals of pSTAT3 and pFAK in both cancer cell lines. Treatment with scFv hSD5 resulted in similar changes in the molecule signaling of both cancer cell lines.

We expressed the complete IgG hSD5 and experimented on endocytosis. After the PDAC cells BxPc-3 were treated with IgG hSD5, they were incubated at 4 °C and 37 °C for 1 h (Fig. 4D). Incubating the cells at 4 °C would cause the cells to enter a resting state. Unlike in the control IgG group, the reactions of the antibodies for recognizing EphA2 occurred on the cell membrane at both 4 °C and 37 °C. When the IgG antibody hSD5 was administered at 37 °C, the antibodies entered the cells through the cell membrane into the cytoplasm (indicated by the red arrow) through endocytosis. These experimental results were similar to the experiments in which ephrinA1 (EphA2 ligand) was administered. Using the Biolayer interferometry analysis, we analyzed the k_{on} and k_{off} parameters of IgG hSD5 targeting the EphA2 protein; the calculated affinity (K_D) of IgG hSD5 was 2.06 nM (Table 1 and Supplementary Fig. 4).

3.6. Humanized IgG hSD5 can inhibit PDAC cell growth in vivo

We used xenograft mice to evaluate the growth inhibitory effect of IgG hSD5 in vivo. In BxPc-3 xenograft mice, compared with the control IgG treatment (which exhibited no inhibitory effect), IgG hSD5-based treatment significantly inhibited the growth of tumors in vivo. The TGI of IgG hSD5 treatment of 2 mg/kg, iv, qwk was 30 %, and that of the treatment with the IgG hSD5 of 20 mg/kg, iv, qwk was 54.3 % (Fig. 5A). In the same experiment, the TGI of gemcitabine (20 mg/kg, iv, biw) was 35.6 %. However, when we combined low-dose IgG hSD5 and gemcitabine, an improved effect was observed, with a TGI of 60 % (Fig. 5B), and no change in the body weight of the mice was observed (Fig. 5C). We performed IHC staining on tissue sections from the removed tumors to observe the expression levels of EphA2 in BxPc-3 tumors and of the cell proliferation marker Ki-67 in the tissues (Fig. 5D). Compared with the results of the control IgG group, the treatment significantly decreased the expression levels of EphA2 and Ki-67 in the tumors. We also used Mia PaCa-2 xenograft mice to determine the inhibitory effect of IgG hSD5 on in vivo tumor growth. After administering 2 mg/kg of IgG hSD5, the TGI was 53.6 %, whereas after administering 20 mg/kg of IgG hSD5, the TGI increased to 67.5 % (Fig. 5E). When the gemcitabine (20 mg/kg) was administered, the TGIs were 39.2 %, respectively (Fig. 5F). However, similarly to the therapeutic effect observed in BxPc-3 tumor-grafted mice, when we administered combination therapy consisting of low-dose IgG hSD5 and gemcitabine, a significant improved effect was observed, and the TGI was 79.3 % (Fig. 5F). No side effects or changes in body weight were observed in mice (Fig. 5G). Observation of the IHC staining of Mia PaCa-2 tumor tissue sections revealed that the expression levels of EphA2 and Ki-67 in the tissue significantly decreased (Fig. 5H). The results demonstrated that the IgG hSD5-targeted EphA2 effectively inhibited the tumor growth in vivo. The actual measurements of the size and weight of the excised tumor grafts also corresponded with the results measured during the antibody hSD5 treatment (Supplementary Fig. 5).

3.7. Epitope definition of antibody hSD5 binding to EphA2 molecule

To allow the isolated antibodies to recognize the activation site on EphA2, we designed discontinuous fragments as immunogens based on a published EphA2 complex structure (Fig. 2A). To determine whether the antibody hSD5 can recognize two antigen fragments simultaneously, we performed peptide synthesis of the two antigen fragments to test the binding reaction of antibody IgG hSD5. The IgG hSD5 exhibited a binding response to the long peptide (EphA2pep_P1P2) linking the two antigen fragments, and IgG hSD5 individually recognized the two synthetic short peptides (EphA2pep_P1 and EphA2pep_P2) (Fig. 6A). In addition, IgG hSD5 did not exhibit a cross-binding reaction to the two irrelevant peptides. The experimental results indicate that the antibody hSD5 binds to the position of the designed antigen fragment and that the antibody hSD5 interacts with both antigen fragments; the interaction with EphA2pep_P1 was stronger than that with EphA2pep_P2, indicating that the conformational epitope on the antibody structure can

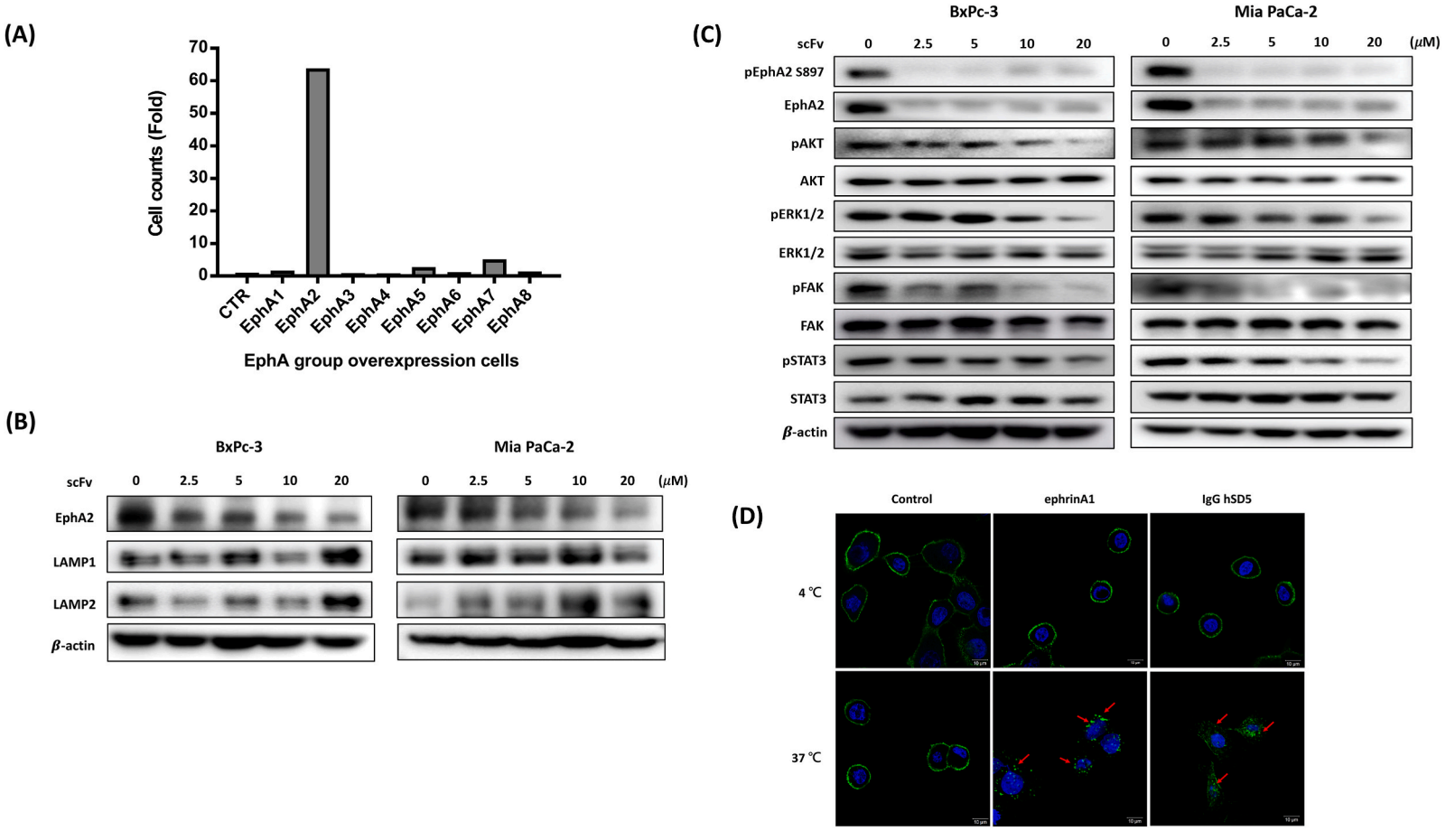

Fig. 4. Binding specificity of humanized antibody hSD5 to EphA2 and induced tumor suppressor molecular signaling. (A) The binding response of humanized scFv hSD5 to different Ephs family proteins was tested through flow cytometry by using the transfected EphA1-A8 overexpression cell line. (B) The scFv SA1 and SD5 interacted with the cancer cells BxPc-3 and Mia PaCa-2 at different concentrations for 6 h, and the degradation reaction of the EphA2 molecule and expression of lysosome-associated markers were observed accordingly. (C) After the cancer cells BxPc-3 and Mia PaCa-2 were treated with different concentrations of humanized scFv hSD5 for 24 h, the cells were lysed, and the molecular signaling in the cell lysate were observed. (D) The resultant endocytosis after the reaction of the humanized IgG hSD5 on the PDAC cells BxPc-3. The test conditions were the cells treated with antibodies and then incubated at 4 °C and 37 °C for 1 h for observation. The ligand ephrin-A1 of EphA2 was used as a positive control for comparison. Control Ab was a commercial anti-EphA2 IgG antibody that could not induce endocytosis. The red arrow indicates that ephrin-A1 and IgG hSD5 are endocytosed from the cell membrane into the cytoplasm.

Table 1
k_{on} and k_{off} rate constants of humanized IgG hSD5 targeting to EphA2 protein.

Ligand	Analyte (IgG)	$k_{on}(10^5\ M^{-1}S^{-1})$	$k_{off}(10^{-4}S^{-1})$	$K_D(10^{-9}M)$
EphA2	hSD5	3.14	6.48	2.06

induce an immune response. In addition, by using the dot blotting assay, we obtained experimental findings similar to the peptide ELISA (Fig. 6B); IgG hSD5 can recognize both the antigen fragments EphA2pep_P1 and EphA2pep_P2, and their binding reaction with the peptide EphA2pep_P1 was stronger than that with EphA2pep_P2.

4. Discussion

Several studies have revealed that EphA2 molecules are highly expressed in PDAC tissues and correlate with the severity of tumorigenesis, which supports the use of EphA2 as a tumor marker for diagnosing and treating PDAC. We observed similar results in tissue array specimens in the present study. In the specimen stained in Fig. 1D, we used a tissue microarray glass slide containing 38 pancreatic carcinomas and 8 normal pancreatic tissues for IHC analysis. Of the 38 cases, 37 were adenocarcinomas with high, moderate, and low levels of differentiation in terms of histopathology. Only one case was classified as squamous cell carcinoma. The careful microscopical investigation by a pathologist revealed that the EphA2 molecules in 34 of the 37 adenocarcinomas were strongly stained in a diffuse, cytoplasmic staining pattern, whereas those for squamous cell carcinoma were entirely negative; focal staining was observed in the acinus areas, but not in the ductal compartment of five of the eight normal pancreatic tissues. In two of the three adenocarcinomas with low levels of differentiation, diffuse, cytoplasmic, and focal and typical membrane staining patterns were observed, suggesting that EphA2 is a membranous biomarker often identified in cancer cells with extremely high histopathological grading. The results indicate that the EphA2 biomarker can be cancer-specific and can be applied for IHC staining for diagnosis and prognostic purposes for adenocarcinomas of the pancreas; it presents a characteristic cytoplasmic staining pattern in most carcinoma cases. For poorly differentiated adenocarcinomas of the pancreas, EphA2 tends to translocate to the cell surface or cell membrane of high-grade cancer cells (Supplementary Fig. 6).

Because the Eph receptor family proteins exhibit abnormal expression and functions in many cancers, researchers have widely investigated this complex family of receptor tyrosine kinases for cancer therapy. Because these receptor proteins are located on the surface of tumor cells within an appropriate microenvironment, they represent a suitable target for therapy. Ephrin A1 can produce a tumor suppressive response through the downregulation induced by its binding to EphA2, which is independent of intercellular contact in the tumor. However, in the tumor microenvironment, ephrin A1 presents decreased concentration and modulation of ephrin A1 was disturbed [19,20]. In the therapeutic strategy targeting EphA2, the use of soluble ephrin A1 or fusing recombinant ephrin A1 to human IgG Fc for dimerization can effectively promote the phosphorylation and degradation of EphA2 and ultimately inhibit the growth of tumor cells [21]. However, ephrin A1 interacts with multiple Eph family molecules, and these factors may produce adverse side effects, limiting its efficacy. There are only two antibody drugs targeting EphA2 that have undergone clinical trials. DS-8895a is a humanized antibody that can enhance antitumor effects when combined with cisplatin [22]. MEDI-547 is an antibody-drug conjugate that induces endocytosis following EphA2 degradation. However, MEDI-547 may have caused bleeding and severe side effects due to insufficient specificity to EphA2, leading to the cessation of its clinical trials [23]. In addition to antibodies, peptide-based therapeutic drugs are also under development. However, these peptide molecules have a binding affinity of approximately 0.1 μM for EphA2. Their shorter half-life and the need for higher effective doses will pose challenges for therapeutic applications [24,25]. Through structural design for immunogens, we prepared specific antibodies targeting the binding of ephrin A1 at the activation site on EphA2; the experimental results indicate that the antibody can bind to the conformational epitope formed by two discontinuous surfaces (Fig. 6). Therefore, the antibody hSD5 can induce a forward tumor growth inhibitory effect similar to ephrin A1 targeting EphA2. The hSD5 binds specifically to EphA2 and does not cross-bind to other Eph family proteins (Fig. 4A). This result reflects the advantages of antibodies: preventing adverse side effects and facilitating inhibitory reactions that neutralize the EphA2 molecule.

Studies have demonstrated that the EphA2 downstream AKT, ERK1/2 signaling pathway regulates tumor growth and the metastasis of glioblastoma, lung cancer cells, and thyroid cancer cells [26–28]. We successfully developed an anti-EphA2 hSD5 monoclonal antibody and targeted the EphA2 receptor on PDAC as a therapeutic strategy. The hSD5 antibody recognized the EphA2 receptor, causing hSD5–EphA2 complex internalization and lysosomal degradation, which led to Ser897 downregulation in BxPc-3 and Mia PaCa-2 PDAC cells (Fig. 7). These results are similar to those obtained in studies that have also used antibodies to target EphA2 molecules and induce the signaling regulation of protein degradation [29], suggesting an association between EphA2 expression and tumor development. We also provide evidence that the oncogenic pERK1/2, pAKT, and pSTAT3 signaling pathways decreased after hSD5 antibody treatment, which inhibited PDAC cell proliferation and migration (Fig. 4C). This result is consistent with ophiopogonin B treatment, which downregulated the EphA2/AKT pathway in lung cancer [27]. These results suggest the feasibility of using the target EphA2 as a cancer treatment.

The humanization is a critical aspect of antibody development. Unstable grafting structures can lead to the inactivation of antibodies and affect their binding ability. We tested the binding of humanized scFv hSD5 to EphA2 molecules after continuous dilution. We observed that the binding (EC_{50}) of humanized scFv hSD5 to EphA2 was superior to that of the original chicken-derived scFv SD5 (Supplementary Fig. 7). We inferred that humanized scFv hSD5 had high structural stability and consequently stronger binding than that of the original chicken-derived scFv SD5. Conversely, inappropriate grafting scaffolds results in unstable structures, which in turn

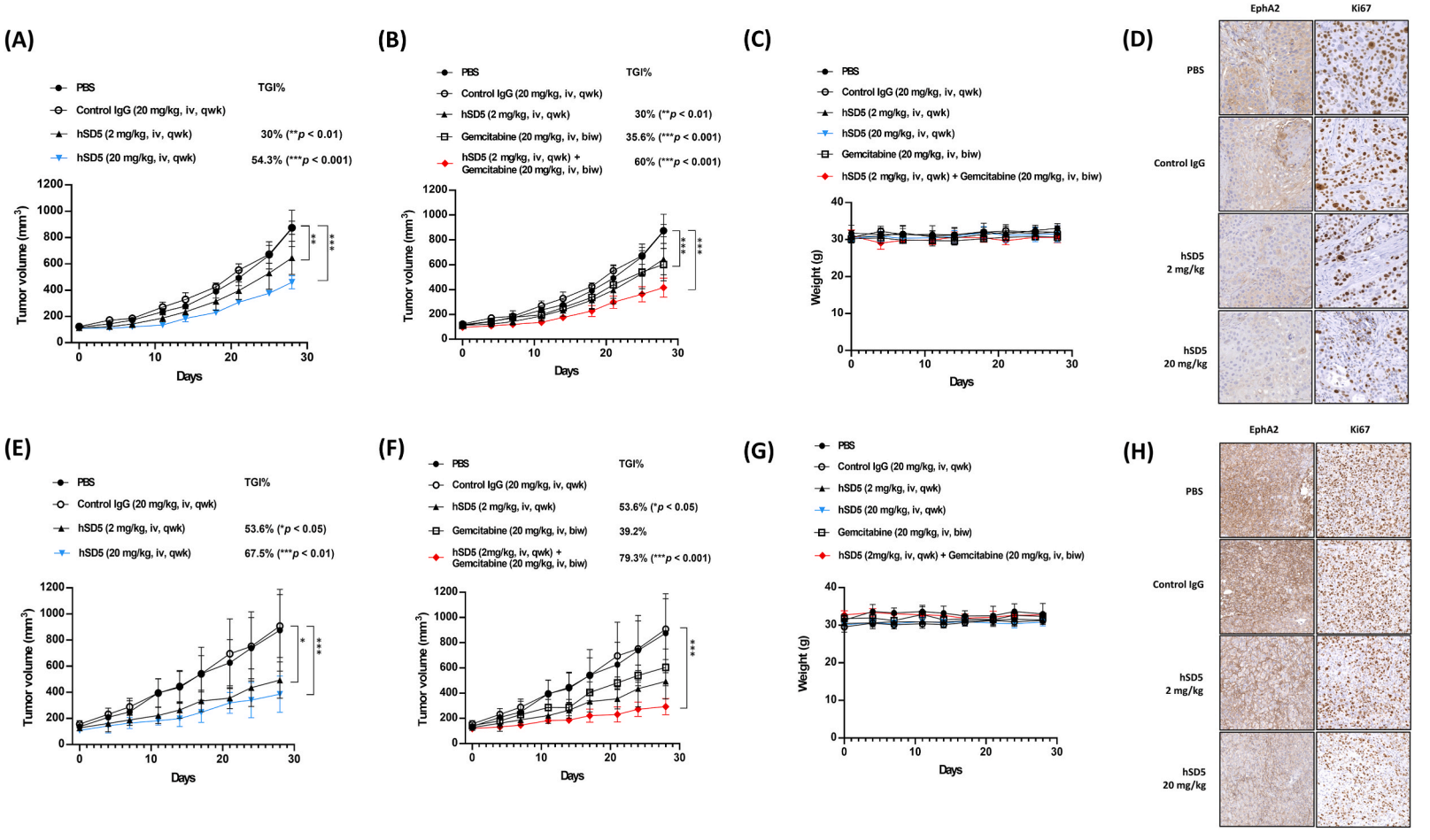

Fig. 5. In vivo tumor growth inhibitory effect of humanized IgG hSD5 on BxPc-3 and Mia PaCa-2 xenograft mice. The growth inhibitory effect of IgG hSD5 (2 mg/kg, iv, qwk, labeled with a solid black triangle and 20 mg/kg, iv, biw, labeled with a solid-blue inverted triangle) on tumor (A) BxPc-3 and (E) Mia PaCa-2 were observed. The growth inhibitory effect of gemcitabine (20 mg/kg, iv, biw, marked with empty black squares) alone, and IgG hSD5 (2 mg/kg) and gemcitabine simultaneously (marked with solid red diamond) on tumor (B) BxPc-3 and (F) Mia PaCa-2. After administering antibodies and small molecules, the weight changes in the (C) BxPc-3 and (G) Mia PaCa-2 xenograft mice were recorded. The expression of EphA2, the cell proliferation marker Ki-67 in the removed (D) BxPc-3 and (H) Mia PaCa-2 tumors were observed using IHC staining. The mouse numbers/per group are n = 6 for the BxPc-3 model and n = 5 for the Mia PaCa-2 model. *$p < 0.05$, **$p < 0.01$, ***$p < 0.001$.

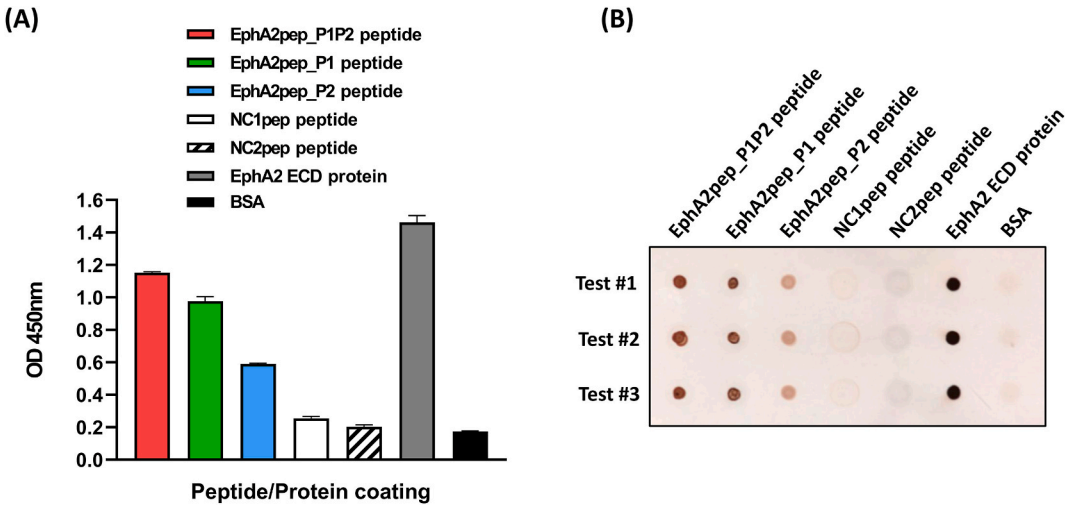

Fig. 6. The IgG hSD5 recognizes epitope at the active site of EphA2. (A) The synthetic peptide was used to perform ELISA to test the binding reaction of the antibody hSD5; the two short peptides at the designed EphA2 activation site were EphA2pep_P1 and EphA2pep_P2. The long peptide formed by linking two short peptides was EphA2pep_P1P2. NC1pep and NC2pep were two irrelevant peptides that acted as the negative controls, whereas EphA2 ECD was a recombinant EphA2 extracellular domain protein. (B) The reaction of antibody hSD5 binding to synthetic peptide was tested through a dot blotting assay.

result in weak antibody binding after humanization (i.e., scFv BSD5 in Supplementary Fig. 7). To determine whether the structural stability of humanized scFv hSD5 was high because of antibody engineering, we used a thermal shift assay to obtain the melting curve of scFv. The results indicate that the TM of chicken-derived scFv SD5 was 75 °C, whereas the melting curve of humanized scFv hSD5 shifted, with a TM of 82 °C (Supplementary Fig. 8). This change in TM indicates that the humanized scFv hSD5 has a more stable structure; antibody stability was not affected by the repulsive interaction between the grafted scaffold and the CDR loops caused by humanized antibody engineering.

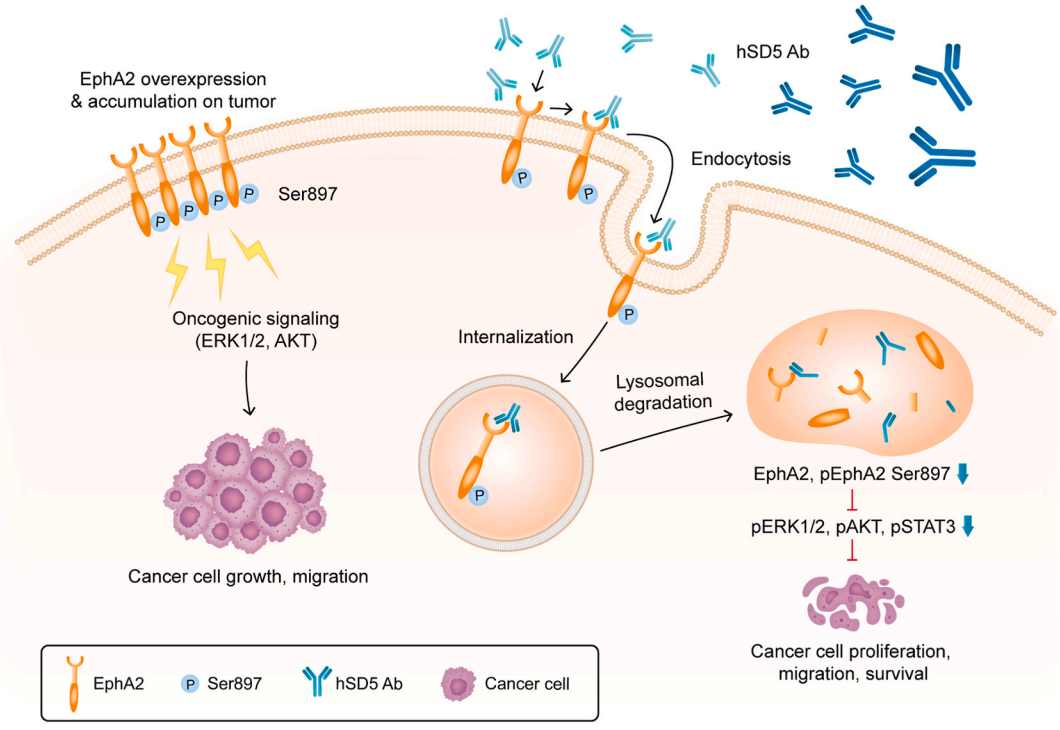

Fig. 7. Schematic of the tumor growth inhibition mechanism caused by the IgG hSD5 targeting EphA2 on the cancer cells.

Target therapy drugs are widely used in clinical cancer treatment. However, the complexity of the tumor microenvironment is a challenge in cancer treatment because single-target therapy often results in tumor tolerance and leads to unsatisfactory results. Cocktail therapy may be an effective solution to resolve this problem. In the in vivo tumor experiment with the antibody hSD5, the administration of hSD5 (2 mg/kg, iv, qwk) in combination with gemcitabine (20 mg/kg, iv, biw) produced improved response like a synergistic effect on the cancer cells BxPc-3 and Mia PaCa-2. These results indicate that using a low dose in combined therapy can result in tumor growth inhibition, and they also indicate the potential of antibody hSD5 for therapeutic applications. Gemcitabine is the first-line treatment drug for pancreatic adenocarcinoma; it can inhibit DNA synthesis after entering cells, resulting in cytotoxicity [30,31]. However, when combined with the inhibitory effect induced by EphA2 on the surface of hSD5-targeted cancer cells, a more comprehensive therapeutic effect can be obtained in PDAC. Therefore, we have planned further experiments for the future, such as combining the antibody with other small molecule drugs or exploring different dosage combination treatment strategies, to investigate the potential induction of a synergistic effect. Another experiment revealed that the binding of the antibody hSD5 to the EphA2 molecule on the surface of cancer cells causes the degradation of the EphA2 molecule and induces endocytosis of the cell, which enables the entry of the antibody molecule into the cytoplasm (Fig. 4C); this is similar to the process of antibodies binding at the EphA2 active site and producing an ephrinA1 targeting–like response. This observation indicates that hSD5 can be developed into an antibody-drug conjugate. In preliminary experiments, we demonstrated that labeling hSD5 with the small molecule of MMAE effectively induces apoptosis in cancer cells (unpublished data), and additional drug efficacy tests are being planned.

5. Conclusion

In this study, the importance of EphA2 for PDAC tumorigenesis has been confirmed. We generated an antibody hSD5 bound to the conformational epitope of endogenous EphA2 on cancer cells, thus inducing cellular endocytosis and causing EphA2 degradation. The treatment turned on a series of downstream inhibition signaling to inhibit the proliferation and migration of pancreatic cancer cells. The antibody hSD5 could effectively inhibit the growth of the xenograft pancreatic cancer tumor cells BxPc-3 and Mia PaCa-2 in mice, respectively. When the antibody was administered with gemcitabine, a significantly improved tumor growth inhibition response was observed. Based on the efficacy of the antibody hSD5, clinical administration of the antibody is likely to suppress tumors in patients with pancreatic cancer and abnormal activation or overexpression of EphA2 signaling.

Ethics approval and consent to participate

The experimental animals in the study were maintained carefully, and all animal experiments were conducted in accordance with ethical standards. The protocols were reviewed and approved by the Animal Use and Management Committee of Taipei Medical University (IACUC number: LAC-2019-0464).

Consent for publication

Not applicable.

Data availability statement

Data will be made available on request.

Funding

This work was financially supported by the “TMU Research Center of Cancer Translational Medicine” from The Featured Areas Research Center Program within the framework of the Higher Education Sprout Project by the Ministry of Education (MOE) in Taiwan and Ministry of Science and Technology in Taiwan under Grant MOST 111-2320-B-038-056.

CRediT authorship contribution statement

Fu-Ling Chang: Writing – original draft, Project administration, Methodology, Investigation, Formal analysis, Data curation, Conceptualization. **Keng-Chang Tsai:** Supervision, Resources, Methodology, Investigation. **Tsai-Yu Lin:** Methodology, Investigation, Formal analysis, Data curation. **Chen-Wei Chiang:** Validation, Formal analysis, Data curation. **Shiow-Lin Pan:** Writing – review & editing, Supervision, Resources, Conceptualization. **Yu-Ching Lee:** Writing – review & editing, Resources, Project administration, Funding acquisition, Conceptualization.

Declaration of competing interest

The authors declare that they have no known competing financial interests or personal relationships that could have appeared to influence the work reported in this paper.

Acknowledgements

We thank Prof. Ann Chen (Department of laboratory medicine of Clinic Pathology, Buddhist Tzu Chi General Hospital, Hualien, Taiwan) for the productive discussions and pathological investigation of the IHC staining in this study.

Appendix A. Supplementary data

Supplementary data to this article can be found online at https://doi.org/10.1016/j.heliyon.2023.e21774.

Abbreviations

Ephs Erythropoietin-producing hepatocyte receptors
EphA2 Erythropoietin-producing hepatocyte receptor type A2
GPI glycosylphosphatidylinositol
PDAC pancreatic cancer
EGF epidermal growth factor
ATCC American Type Culture Collection
NOD/SCID nonobese diabetic mice with severe combined immunodeficiency
GEPIA Gene Expression Profiling Interactive Analysis
TMB 3,5,5-tetramethubezidine dihydrochloride
FITC fluorescein isothiocyanate
HA hemagglutinin
MTS 3-(4,5-dimethylthiazol-2-yl)-5-(3-carboxymethoxyphenyl)-2-(4-sulfophenyl)-2H-tetrazolium
TGI tumor growth inhibition
IHC immunohistochemical staining
ELISA enzyme-linked immunosorbent assay
PBST phosphate-buffered saline with 0.05 % Tween 20
HRP horseradish peroxidase
SDS-PAGE sodium dodecyl sulfate–polyacrylamide gel
Native-PAGE native-polyacrylamide gel

References

[1] H. Hirai, Y. Maru, K. Hagiwara, J. Nishida, F. Takaku, A novel putative tyrosine kinase receptor encoded by the eph gene, Science 238 (4834) (1987) 1717–1720.
[2] E.M. Lisabeth, G. Falivelli, E.B. Pasquale, Eph receptor signaling and ephrins, Cold Spring Harb Perspect Biol 5 (9) (2013).
[3] J.P. Himanen, M.J. Chumley, M. Lackmann, C. Li, W.A. Barton, P.D. Jeffrey, C. Vearing, D. Geleick, D.A. Feldheim, A.W. Boyd, M. Henkemeyer, D.B. Nikolov, Repelling class discrimination: ephrin-A5 binds to and activates EphB2 receptor signaling, Nat. Neurosci. 7 (5) (2004) 501–509.
[4] A. Lodola, C. Giorgio, M. Incerti, I. Zanotti, M. Tognolini, Targeting Eph/ephrin system in cancer therapy, Eur. J. Med. Chem. 142 (2017) 152–162.
[5] E.P. Sulman, X.X. Tang, C. Allen, J.A. Biegel, D.E. Pleasure, G.M. Brodeur, N. Ikegaki, ECK, a human EPH-related gene, maps to 1p36.1, a common region of alteration in human cancers, Genomics 40 (2) (1997) 371–374.
[6] A.W. Boyd, P.F. Bartlett, M. Lackmann, Therapeutic targeting of EPH receptors and their ligands, Nat. Rev. Drug Discov. 13 (1) (2014) 39–62.
[7] D.P. Zelinski, N.D. Zantek, J.C. Stewart, A.R. Irizarry, M.S. Kinch, EphA2 overexpression causes tumorigenesis of mammary epithelial cells, Cancer Res. 61 (5) (2001) 2301–2306.
[8] M.S. Kinch, M.B. Moore, D.H. Harpole Jr., Predictive value of the EphA2 receptor tyrosine kinase in lung cancer recurrence and survival, Clin. Cancer Res. 9 (2) (2003) 613–618.
[9] J. Wykosky, D.M. Gibo, C. Stanton, W. Debinski, EphA2 as a novel molecular marker and target in glioblastoma multiforme, Mol. Cancer Res. 3 (10) (2005) 541–551.
[10] S.V. Mudali, B. Fu, S.S. Lakkur, M. Luo, E.E. Embuscado, C.A. Iacobuzio-Donahue, Patterns of EphA2 protein expression in primary and metastatic pancreatic carcinoma and correlation with genetic status, Clin. Exp. Metastasis 23 (7–8) (2006) 357–365.
[11] H. Miao, N.W. Gale, H. Guo, J. Qian, A. Petty, J. Kaspar, A.J. Murphy, D.M. Valenzuela, G. Yancopoulos, D. Hambardzumyan, J.D. Lathia, J.N. Rich, J. Lee, B. Wang, EphA2 promotes infiltrative invasion of glioma stem cells in vivo through cross-talk with Akt and regulates stem cell properties, Oncogene 34 (5) (2015) 558–567.
[12] P. Kaenel, M. Mosimann, A.C. Andres, The multifaceted roles of Eph/ephrin signaling in breast cancer, Cell Adh Migr 6 (2) (2012) 138–147.
[13] H. Miao, D.Q. Li, A. Mukherjee, H. Guo, A. Petty, J. Cutter, J.P. Basilion, J. Sedor, J. Wu, D. Danielpour, A.E. Sloan, M.L. Cohen, B. Wang, EphA2 mediates ligand-dependent inhibition and ligand-independent promotion of cell migration and invasion via a reciprocal regulatory loop with Akt, Cancer Cell 16 (1) (2009) 9–20.
[14] A. Van den Broeck, H. Vankelecom, R. Van Eijsden, O. Govaere, B. Topal, Molecular markers associated with outcome and metastasis in human pancreatic cancer, J. Exp. Clin. Cancer Res. 31 (2012) 68.
[15] R.L. Siegel, K.D. Miller, A. Jemal, Cancer Statistics, 2017, CA Cancer J Clin 67 (1) (2017) 7–30.
[16] Z. Tang, C. Li, B. Kang, G. Gao, C. Li, Z. Zhang, GEPIA: a web server for cancer and normal gene expression profiling and interactive analyses, Nucleic Acids Res. 45 (W1) (2017) W98–W102.
[17] J. Andris-Widhopf, C. Rader, P. Steinberger, R. Fuller, C.F. Barbas 3rd, Methods for the generation of chicken monoclonal antibody fragments by phage display, J. Immunol. Methods 242 (1–2) (2000) 159–181.
[18] C.F. Barbas 3rd, A.S. Kang, R.A. Lerner, S.J. Benkovic, Assembly of combinatorial antibody libraries on phage surfaces: the gene III site, Proc Natl Acad Sci U S A 88 (18) (1991) 7978–7982.

[19] V.M. Youngblood, L.C. Kim, D.N. Edwards, Y. Hwang, P.R. Santapuram, S.M. Stirdivant, P. Lu, F. Ye, D.M. Brantley-Sieders, J. Chen, The ephrin-A1/EPHA2 signaling Axis regulates glutamine metabolism in HER2-positive breast cancer, Cancer Res. 76 (7) (2016) 1825–1836.
[20] K. Ieguchi, Y. Maru, Roles of EphA1/A2 and ephrin-A1 in cancer, Cancer Sci. 110 (3) (2019) 841–848.
[21] M.S. Duxbury, H. Ito, M.J. Zinner, S.W. Ashley, E.E. Whang, Ligation of EphA2 by Ephrin A1-Fc inhibits pancreatic adenocarcinoma cellular invasiveness, Biochem. Biophys. Res. Commun. 320 (4) (2004) 1096–1102.
[22] J. Hasegawa, M. Sue, M. Yamato, J. Ichikawa, S. Ishida, T. Shibutani, M. Kitamura, T. Wada, T. Agatsuma, Novel anti-EPHA2 antibody, DS-8895a for cancer treatment, Cancer Biol. Ther. 17 (11) (2016) 1158–1167.
[23] D. Jackson, J. Gooya, S. Mao, K. Kinneer, L. Xu, M. Camara, C. Fazenbaker, R. Fleming, S. Swamynathan, D. Meyer, P.D. Senter, C. Gao, H. Wu, M. Kinch, S. Coats, P.A. Kiener, D.A. Tice, A human antibody-drug conjugate targeting EphA2 inhibits tumor growth in vivo, Cancer Res. 68 (22) (2008) 9367–9374.
[24] M. Koolpe, M. Dail, E.B. Pasquale, An ephrin mimetic peptide that selectively targets the EphA2 receptor, J. Biol. Chem. 277 (49) (2002) 46974–46979.
[25] M. Koolpe, R. Burgess, M. Dail, E.B. Pasquale, EphB receptor-binding peptides identified by phage display enable design of an antagonist with ephrin-like affinity, J. Biol. Chem. 280 (17) (2005) 17301–17311.
[26] Y. Hamaoka, M. Negishi, H. Katoh, EphA2 is a key effector of the MEK/ERK/RSK pathway regulating glioblastoma cell proliferation, Cell. Signal. 28 (8) (2016) 937–945.
[27] M. Chen, C. Hu, Y. Guo, R. Jiang, H. Jiang, Y. Zhou, H. Fu, M. Wu, X. Zhang, Ophiopogonin B suppresses the metastasis and angiogenesis of A549 cells in vitro and in vivo by inhibiting the EphA2/Akt signaling pathway, Oncol. Rep. 40 (3) (2018) 1339–1347.
[28] C. Allocca, A.M. Cirafici, M.O. Laukkanen, M.D. Castellone, Serine 897 phosphorylation of EPHA2 is involved in signaling of oncogenic ERK1/2 drivers in thyroid cancer cells, Thyroid 31 (1) (2021) 76–87.
[29] H. Ansuini, A. Meola, Z. Gunes, V. Paradisi, M. Pezzanera, S. Acali, C. Santini, A. Luzzago, F. Mori, D. Lazzaro, G. Ciliberto, A. Nicosia, N. La Monica, A. Vitelli, Anti-EphA2 antibodies with distinct in vitro properties have equal in vivo efficacy in pancreatic cancer, J Oncol 2009 (2009), 951917.
[30] H.A. Burris 3rd, M.J. Moore, J. Andersen, M.R. Green, M.L. Rothenberg, M.R. Modiano, M.C. Cripps, R.K. Portenoy, A.M. Storniolo, P. Tarassoff, R. Nelson, F. A. Dorr, C.D. Stephens, D.D. Von Hoff, Improvements in survival and clinical benefit with gemcitabine as first-line therapy for patients with advanced pancreas cancer: a randomized trial, J. Clin. Oncol. 15 (6) (1997) 2403–2413.
[31] E. Moysan, G. Bastiat, J.P. Benoit, Gemcitabine versus Modified Gemcitabine: a review of several promising chemical modifications, Mol. Pharm. 10 (2) (2013) 430–444.